Materials and Design 36 (2012) 443–450

Contents lists available at SciVerse ScienceDirect

Materials and Design

journal homepage: www.elsevier.com/locate/matdes

Technical Report

Influence of grain refining elements on mechanical properties of AISI 430 ferritic stainless steel weldments – Taguchi approach

G. Mallaiah [a,*], A. Kumar [b], P. Ravinder Reddy [c], G. Madhusudhan Reddy [d]

[a] Department of Mechanical Engineering, KITS, Singapur, Huzurabad, A.P., India
[b] Department of Mechanical Engineering, NIT, Warangal, A.P., India
[c] Department of Mechanical Engineering, CBIT, Gandipet, Hyderabad, A.P., India
[d] Defence Metallurgical Research Laboratory, Hyderabad, A.P., India

ARTICLE INFO

Article history:
Received 18 October 2011
Accepted 26 November 2011
Available online 8 December 2011

ABSTRACT

The effect of grain refining elements such as copper, titanium and aluminum on transverse tensile strength, ductility, impact toughness, microhardness and austenite content of AISI 430 ferritic stainless steel welds through Gas Tungsten Arc Welding (GTAW) process in as-welded condition was studied. Taguchi method was used to optimize the weight percentage of copper, titanium and aluminum for maximizing the mechanical properties and austenite content in the weld region of ferritic stainless steel welds. Based on Taguchi orthogonal array the regression equations were developed for predicting the mechanical properties of ferritic stainless steel welds within the range of grain refining elements. The observed mechanical properties and austenite content have been correlated with microstructure and fracture features.

1. Introduction

Ferritic stainless steel (FSS) is characterized by lower cost, higher thermal conductivity, smaller linear expansion and better resistance to chloride stress corrosion cracking, atmospheric corrosion and oxidation compared to austenitic stainless steels [1,2]. In certain applications such as the production of titanium by kroll process, where titanium tetrachloride ($TiCl_4$) is reduced by magnesium, austenitic stainless steels are used for the reduction retorts with an inner lining of FSS to mitigate the problem of leaching of the nickel by molten magnesium. These steels are extensively used in making vessels for food and chemical industries, heat exchangers, architectural and automotives, etc. Gas Tungsten Arc Welding (GTAW) or Tungsten Inert Gas (TIG) welding is an arc welding process that produces coalescence of metals by heating them with an arc between a non-consumable electrode and the base metal. GTAW process is well suitable for joining thin and medium thickness material like aluminum alloys and steels. GTAW process is generally used for welding of these alloys because it produces very high quality welds [3].

The principle weldability issue with the FSS is maintaining adequate toughness and ductility in the weld zone (WZ) and heat affected zone (HAZ) of these steels, this is due to large grain size in the fusion zone (FZ) [4–6] because they solidify directly from the liquid to the ferrite phase without any intermediate phase transformation. The problem of grain coarsening in the WZ of FSS welds is addressed by limiting heat input by employing low heat input welding processes [7–10]. Strong carbide and nitride forming elements are usually added to eliminate the sensitization and improve the mechanical properties of FSS [11–15]. Studies have been conducted to grain refine FSS welds by electromagnetic stirring [16], by employing alternating current GTAW process [17–19] as well as through liquid metal chilling [20]. Earlier attempts have been made to grain refine welds of these steels by the addition of elements such as titanium and copper [21]. From the reported literature it is observed that the grain refinement in the WZ of AISI 430 FSS welds by the addition of grain refining elements such as copper (Cu), titanium (Ti) and aluminum (Al) with specified weight percentage for increasing the mechanical properties is not studied and also it is observed that the optimization of grain refining elements in the WZ of AISI 430 FSS welds for maximizing the mechanical properties is not reported.

Factorial design of experiments using Taguchi method is a systematic method of approach for design and analysis of experiments for the purpose of improving the quality characteristics [22–25]. Nowadays, Taguchi method has become a practical tool for improving the quality of output without increasing the cost of experimentation by reducing the number of experiments. Juang and Tarang [26] have used Taguchi method for optimizing the process parameters of TIG welding of stainless steel. They have used arc gap, flow rate, welding current and welding speed each with four levels for optimization of weld pool geometry. Kumar and Sundarrajan [27] optimized mechanical properties of TIG welded Al–Mg–Si aluminum alloy using Taguchi method. Balasubramanian et al. [28]

* Corresponding author. Tel.: +91 9440324639; fax: +91 8727 252744.
E-mail addresses: gmallaiah_kits@yahoo.co.in, gmh.me@kitssingapuram.com (G. Mallaiah).

0261-3069/$ - see front matter © 2011 Elsevier Ltd. All rights reserved.
doi:10.1016/j.matdes.2011.11.063

obtained refined grain size with pulsed current TIG welding of aluminum alloys to Ti alloys. They have used peak current, base current, pulse frequency and pulse on-time as the process parameters with four levels for optimizing the three quality characteristics of tensile, notch tensile and yield strengths.

The objective of the present study is to investigate the influence of grain refining elements such as Cu, Ti and Al addition on mechanical properties of AISI 430 FSS weldments and to obtain the optimum combinations of these grain refining elements for increasing the mechanical properties and austenite content using Taguchi method.

2. Experimental procedure

The base material employed in this study is 5 mm thick AISI 430 FSS. The chemical composition of the base material is presented in Table 1. GTAW was carried out using a Master TIG AC/DC 3500W welding machine (Make: kemppi). The advantages of the GTAW process are low heat input, less distortion, resistance to hot cracking and better control of FZ there by improved mechanical properties. From the reported literature [7–10] and previous work done [21], the most important process parameters which are having greater influence on the weld bead geometry and FZ grain refinement of continuous current GTAW process have been identified. They are as: welding current, welding speed and arc voltage. In the present investigation, trial runs were conducted by varying the weight percentage of one of the grain refining elements and keeping the others constant to find the working range of grain refining elements. Feasible levels of the grain refining elements were chosen in such a way that the joint should be free from any visible defects.

The range of the grain refining elements selected under the present study and the constant process parameters are presented in Tables 2 and 3 respectively. In the present study, the Taguchi method was applied to experimental data using statistical software Minitab 15. The number of grain refining elements considered under this study is three and the level of each grain refining element is three. The degree of freedom of all the three grain refining elements is 6. Hence, L_9 (3^4) orthogonal array is selected. Each condition of experiment was repeated twice to reduce the noise/error effects. The details of the selected orthogonal array were presented in Table 4. The S/N ratio for each level of the grain refining element is computed.

The quality characteristics, i.e. ultimate tensile strength (UTS), yield strength (YS), impact toughness (IT), percentage of elongation (%EL), microhardness and austenite content of the welds were evaluated for all the trials and then statistical analysis of variance (ANOVA) was carried out. Based on the ANOVA, the contribution of each element in influencing the quality characteristic is evaluated. The ANOVA also provides an indication of which elements are statistically significant. The optimum elements combination are predicted and verified.

The rolled plates of 5 mm thick AISI 430 FSS were cut into the required dimension. A single 'V' butt joint configuration shown in Fig. 1 was selected and the joints were made using the experimental layout shown in Table 4. Prior to welding, the base metal plates were wire brushed and degreased using acetone and preheated to 100 °C. All the necessary care was taken to avoid the joint distortion during welding. Purging is provided at the bottom of the plates. The same argon gas is used for shielding as well as purging. A filler material conforming to the composition given in Table 1 is used. Cu (in foil form) was added between the butt joint of FSS after the root weld. Then, Ti and Al powders of −100 μm mesh (99% purity level) were added to the molten pool through hopper and a fine pipe by the controlled way using the motor mechanism. Weld joint is completed in three passes.

Table 2
Working range of the grain refining elements.

Symbol	Element	Units	Lower level (1)	Medium level (2)	Higher level (3)
A	Copper	g	1	2	3
B	Titanium	g	1	2	3
C	Aluminum	g	1	2	3

Table 3
Constant process parameters.

Parameter	Value
Welding current (Amps)	120
Welding speed (mm/min)	50
Electrode polarity	DCSP
Arc voltage (V)	10–13
Arc gap (mm)	2
Filler wire diameter (mm)	1.6
Electrode	2% Thoriated tungsten
No. of passes	3
Shielding gas (argon), flow rate (L/min)	10
Purging gas (argon) flow rate (L/min)	5
Preheat temperature (°C)	100

Table 4
Experimental layout L_9 (3^4) orthogonal array.

Exp. no.	A	B	C
FS1	1	1	1
FS2	1	2	2
FS3	1	3	3
FS4	2	1	2
FS5	2	2	3
FS6	2	3	1
FS7	3	1	3
FS8	3	2	1
FS9	3	3	2

2.1. Metallography

In order to observe the microstructure under the optical microscope, specimens were cut from the welds, then prepared according to the standard procedures and etched using aquaregia (1 part HNO_3, 3 parts HCL). Microstructures of the welds were studied and recorded. Scanning Electron Microscope (SEM) was used for energy dispersive X-ray analysis (EDX) and fractographic examination. American stress technologies (ASTs) 2000 X-ray stress analyzer

Table 1
Chemical composition of the base material and filler material (wt%).

Material	C	Mn	Si	P	S	Ni	Cr	Fe
Base material (AISI 430 FSS)	0.044	0.246	0.296	0.023	0.002	0.164	17.00	Balance
Filler material (AISI 430 FSS)	0.044	0.246	0.296	0.023	0.002	0.164	17.00	Balance

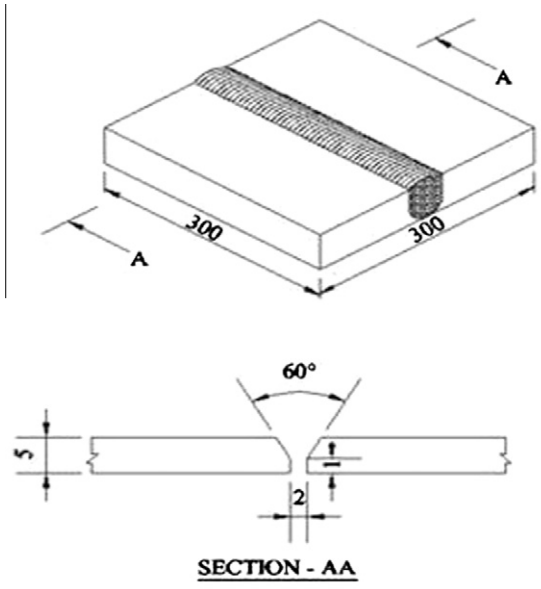

Fig. 1. Schematic sketch of the weld joint (all dimensions are in 'mm').

with a provision to determine austenite was utilized for the measurement of austenite content in the weld region of FSS joints.

2.2. Mechanical testing

Microhardness tests were carried out using a Vickers digital microhardness tester in transverse direction of the weld joint. A load of 300 g was applied for duration of 10 s. The microhardness was measured at an interval of 0.1 mm across the weld, 0.5 mm across the HAZ and unaffected base metal. The schematic sketch of the hardness survey is shown in Fig. 2.

The tensile test specimens were made as per ASTM E8 standards [29] by cutting the welded joints and machined by Wire cut Electrical Discharge Machining (WEDM) to the required dimensions. The configuration of the tensile test specimen adopted is given in Fig. 3. The tensile test was conducted with the help of a computer controlled universal testing machine (Model: TUE-C-600) at a cross

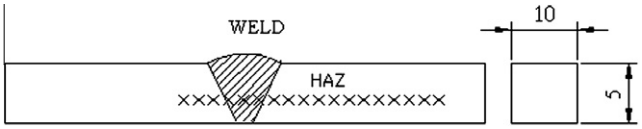

Fig. 2. Schematic sketch of hardness survey across the joint (all dimensions are in 'mm').

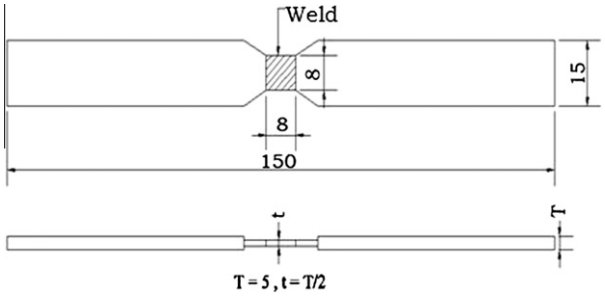

Fig. 3. Configuration of tensile test specimen (all dimensions are in 'mm').

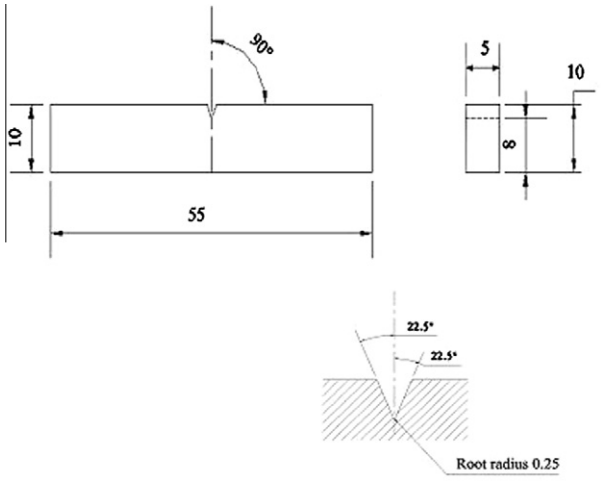

Fig. 4. Configuration of charpy V-notch impact specimen (all dimensions are in 'mm').

head speed of 0.5 mm/min. During tensile tests, all the welded specimens were failed within the weld region.

Charpy impact test specimens were prepared to the dimensions shown in Fig. 4 to evaluate the impact toughness of the weld metal. Since the thickness of the plate was small, subsize [29] specimens were prepared. The impact test was conducted at room temperature using a pendulum type charpy impact testing machine.

3. Results and discussion

3.1. Mechanical properties

The measured values of UTS, YS, %EL, IT, microhardness and austenite content of FSS weldments and base metal were presented in Table 5. The data on all the properties of weldments have been subjected to regression analysis. The responses Y such as UTS, YS, %EL, IT, microhardness and austenite content are the function of Cu, Ti and Al. The response function can be expressed as:

$$Y = f(\mathrm{Cu}, \mathrm{Ti}, \mathrm{Al})$$

$$Y = f(\mathrm{A}, \mathrm{B}, \mathrm{C})$$

For the three factors, the selected polynomial (regression) could be expressed as:

$$Y = b_0 + b_1\mathrm{A}^2 + b_2\mathrm{A} + b_3\mathrm{B}^2 + b_4\mathrm{B} + b_5\mathrm{C}^2 + b_6\mathrm{C} \quad (1)$$

where b_0 is the free term of the regression Eq. (1), the coefficients b_1, b_3 and b_5 are quadratic terms and b_2, b_4 and b_6 are linear terms. The coefficients of the variables are calculated for different responses [30,31]. After determining the coefficients, the regression equations were developed. These equations were used to predict the UTS, YS, IT, %EL, microhardness and austenite content within the factorial space exploited. Regression equations showing the effect of grain refining elements (Cu, Ti and Al) on mechanical properties, austenite content and correlation coefficients for the observed properties and austenite content are summarized in Table 6. High correlation coefficients indicate a good relationship between the grain refining elements (Cu, Ti and Al) and the observed property data. Microhardness survey in transverse to the weld direction of a typical weld (FS8) revealed three different regions, such as WZ, HAZ and unaffected base metal which is shown in Fig. 5. The hardness was highest in the WZ compared to HAZ and unaffected base metal [25,32]. Maximum hardness in the WZ can be attributed to the existence of fine precipitates such as titanium carbides (TiC) and aluminum

Table 5
Mechanical properties and austenite content of AISI 430 FSS weldments.

Specimen ID	UTS (MPa)		YS (MPa)		%EL		IT (J)		Microhardness at the weld center (HV)		Austenite content at the weld region (wt%)	
	Trial 1	Trial 2	Trial 1	Trial 2	Trial 1	Trial 2	Trial 1	Trial 2	Trial 1	Trial 2	Trial 1	Trial 2
FS1	394	395	295	312	4.4	3.9	2	4	235	240	9	9.5
FS2	350	355	235	250	3.6	3.4	4	2	260	265	11.5	10
FS3	364	371	264	225	3.7	3.4	2	2	258	260	9.5	7
FS4	330	335	260	220	3.3	3.4	2	4	235	240	11.5	10.5
FS5	362	365	227	345	3.8	4.6	4	4	270	280	12.5	11.5
FS6	345	354	291	330	4.5	3.8	4	4	280	285	12	12.5
FS7	427	423	265	320	4.7	3.5	4	2	290	310	12.5	14
FS8	491	446	375	395	5.8	6.4	6	6	360	365	19	18
FS9	350	340	225	245	3.8	3.6	4	4	310	320	13.5	12
Base material	426	422	320	316	15	11	20	24	218	222	–	–

Table 6
Regression equations for the mechanical properties and austenite content of AISI 430 FSS weldments.

S. no.	Response	Regression equation	Coefficient of correlation
1	UTS (MPa)	$Y = 352.49 + 43.66 * X_1^2 + 20.66 * X_1 - 25.83 * X_2^2 - 15 * X_2 + 51.41 * X_3^2 - 9.41 * X_3$	0.96
2	YS (MPa)	$Y = 258.19 + 4.99 * X_1^2 + 20.33 * X_1 - 33.49 * X_2^2 - 7.66 * X_2 + 64.5 * X_3^2 - 29.33 * X_3$	0.99
3	%EL	$Y = 3.83 + 0.28 * X_1^2 + 0.45 * X_1 - 0.76 * X_2^2 - 0.03 * X_2 + 0.85 * X_3^2 - 0.42 * X_3$	0.97
4	IT (J)	$Y = 4.21 - 0.16 * X_1^2 + 0.83 * X_1 - 1.16 * X_2^2 + 0.16 * X_2 + 0.33 * X_3^2 - 0.66 * X_3$	0.97
5	Microhardness (HV)	$Y = 287.94 + 5.91 * X_1^2 + 35.41 * X_1 - 24.08 * X_2^2 + 17.08 * X_2 + 15.16 * X_3^2 - 9.83 * X_3$	0.98
6	Austenite content (wt%)	$Y = 13 + 0.375 * X_1^2 + 2.7 * X_1 - 2.62 * X_2^2 - 0.04 * X_2 + 0.75 * X_3^2 - 1.08 * X_3$	0.98

Where X_1 = copper, X_2 = titanium and X_3 = aluminum.

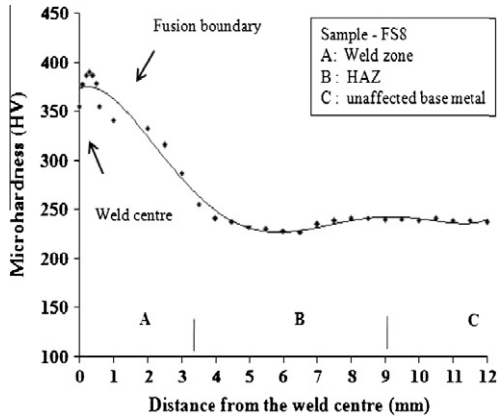

Fig. 5. Microhardness survey in transverse to the weld direction of FSS weld (sample-FS8).

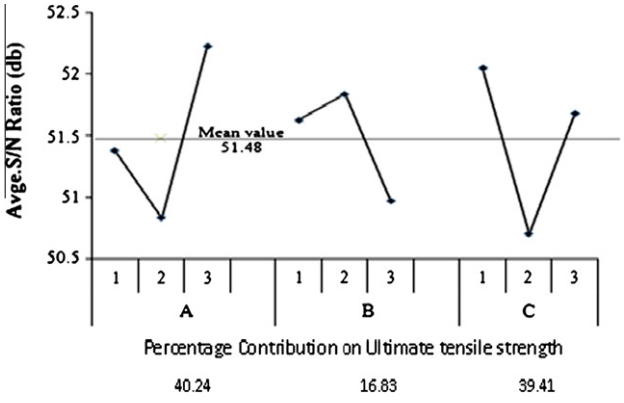

Fig. 6. Graphical representation of S/N ratio and percentage contribution of grain refining elements (Cu, Ti and Al) on UTS.

oxides (Al_2O_3) and solid solution strengthening by the Al during welding.

3.2. Optimization of grain refining elements

The grain refining elements such as Ti and Al were added as powders of −100 μm mesh (99% purity level) to the molten pool in the range from 1 g to 3 g with respect to the weld speed and at a controlled feed rate over a length of 300 mm of the FSS joints and Cu (in foil form) was added between the butt joint of FSS over a length of 300 mm in the range from 1 g to 3 g after the root weld. The weight percentage of grain refining elements Cu, Ti and Al were measured by Electron Probe Microanalysis (EPMA) and it was found that, for the addition of grain refining elements such as Cu (1–3 g) between the butt joint; Ti and Al (1–3 g) to the molten pool, the weight percentage is varying from 0.1 wt% to 0.25 wt% for Cu, 0.3–0.9 wt% for Ti, 1.7–6.2 wt% for Al respectively.

The optimization of weight percentage of grain refining elements using Taguchi method permits evaluation of the effects of individual elements independent of other elements on the identified quality characteristics, i.e. UTS, YS, %EL, IT, microhardness and austenite content [31]. The influence of each grain refining element can be evaluated by determining the S/N ratio for each factor at each level. In this study, for UTS, YS, %EL, IT, microhardness and austenite content, the S/N ratios were chosen according to the criterion of larger-the-better (LB). The S/N ratio (η), on the LB basis for maximizing the selected quality character is calculated as:

$$\eta = -10\log_{10}\left\{\frac{1}{n}\sum_{i=1}^{n}\frac{1}{y_i^2}\right\} \quad (2)$$

where 'y' is the average quality character and 'n' is the number of repetitions. In this study n is equal to 9. Using Eq. (2) and the data

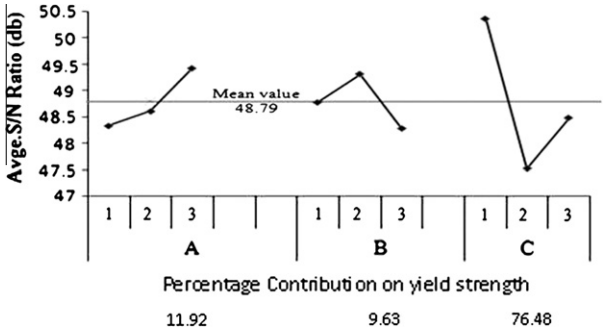

Fig. 7. Graphical representation of S/N ratio and percentage contribution of grain refining elements (Cu, Ti and Al) on YS.

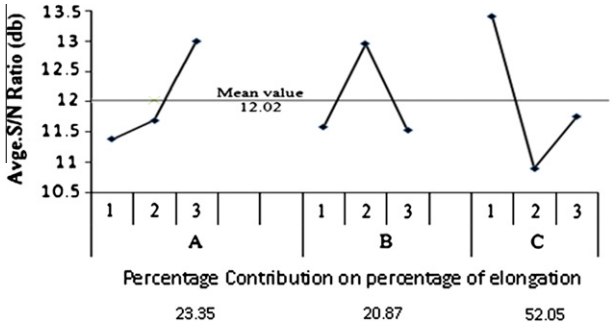

Fig. 8. Graphical representation of S/N ratio and percentage contribution of grain refining elements (Cu, Ti and Al) on %EL.

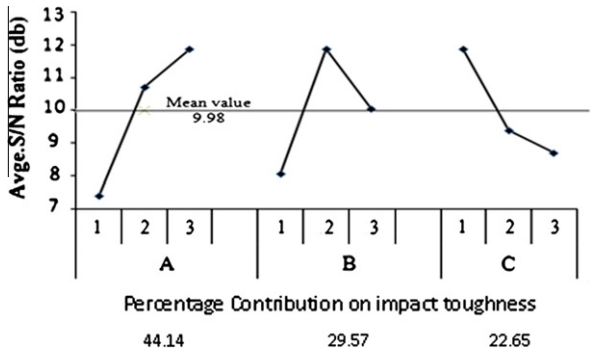

Fig. 9. Graphical representation of S/N ratio and percentage contribution of grain refining elements (Cu, Ti and Al) on IT.

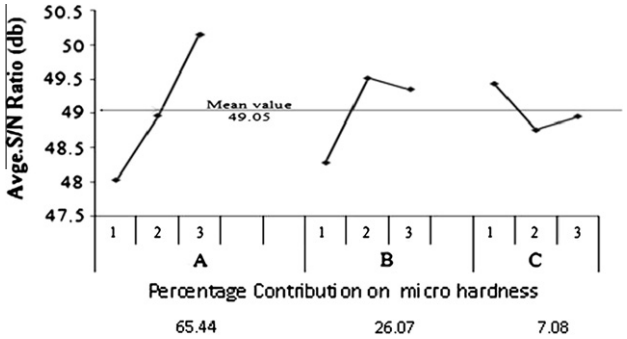

Fig. 10. Graphical representation of S/N ratio and percentage contribution of grain refining elements (Cu, Ti and Al) on microhardness.

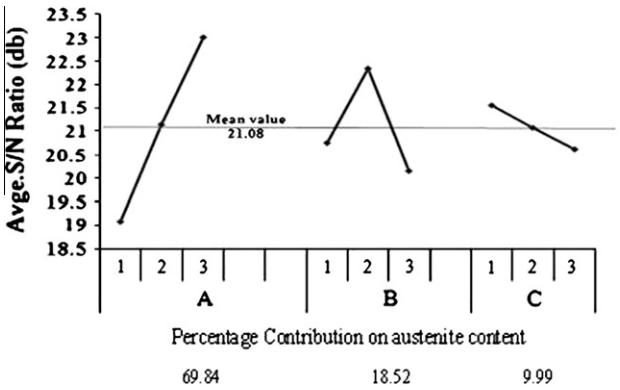

Fig. 11. Graphical representation of S/N ratio and percentage contribution of grain refining elements (Cu, Ti and Al) on austenite content.

Table 7
Optimum values of the quality characteristics.

Quality characteristics	Optimum condition	Optimum value
UTS (MPa)	$A_3B_2C_1$, i.e. Cu at level 3 (3 g), Ti at level 2 (2 g) and Al at level 1 (1 g)	455
YS (MPa)		377
%EL		5.8
IT (J)		6
Microhardness (HV)		359
Austenite content (wt%)		18.32

Table 8
Validation of the optimum results.

Quality characteristics	Optimum condition	Optimum value	Experimental value[a]
UTS (MPa)	$A_3B_2C_1$, i.e. Cu at level 3 (3 g), Ti at level 2 (2 g) and Al at level 1 (1 g)	455	468.5
YS (MPa)		377	385
%EL		5.8	6.1
IT (J)		6	6
Microhardness (HV)		359	362.5
Austenite content (wt%)		18.32	18.5

[a] Average of two values.

presented above, the S/N ratios were calculated. S/N ratio and the percentage contribution of grain refining elements (Cu, Ti and Al) on the quality characteristics such as UTS, YS, %EL, IT, microhardness and austenite content were presented in graphical form in Figs. 6–11. It is observed that the percentage contribution of Cu is more compared to Ti and Al on mechanical properties and austenite content of FSS welds. The optimum results were presented in Table 7. For validations of the optimum results, experiments were conducted as per the optimum conditions, austenite content and mechanical properties were evaluated and the average results are presented in Table 8. It is observed that experimental values were closer to the optimum values. Results of ANOVA indicate that the grain refining elements (Cu, Ti and Al) are significant for all the quality characteristics. The same optimum combination is observed in UTS, YS, %EL, IT, microhardness and austenite content.

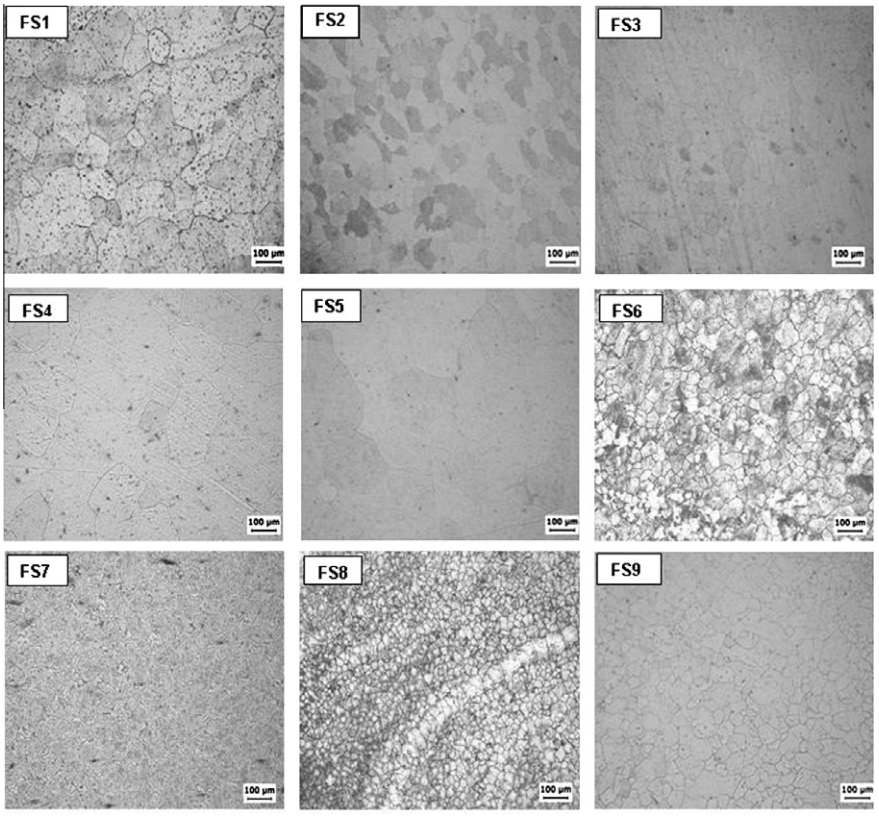

Fig. 12. Microstructures of weld region of FSS welds.

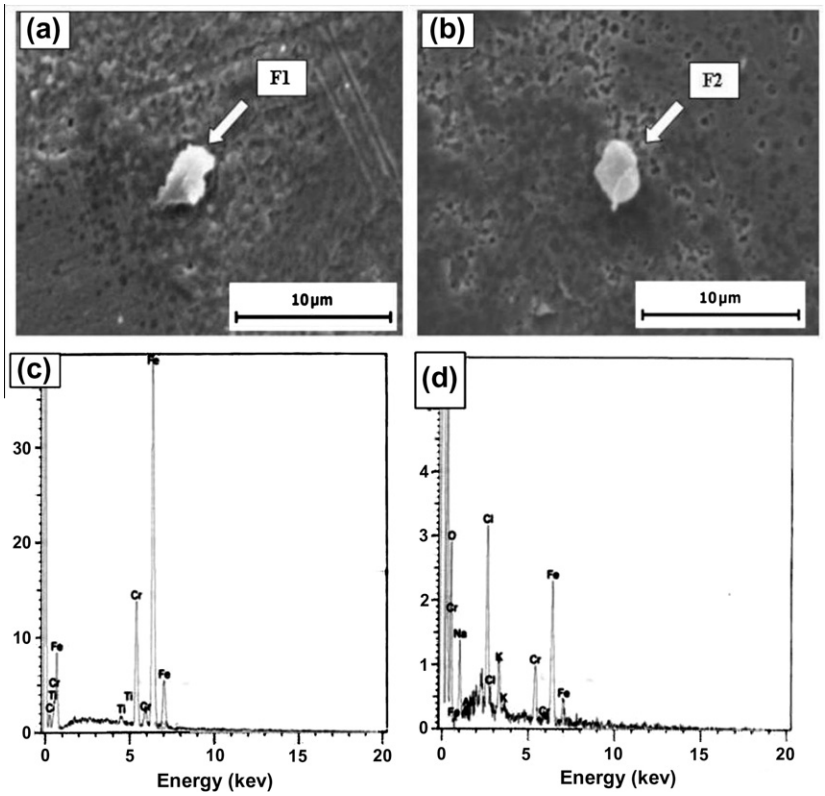

Fig. 13. SEM micrographs (a and b) for precipitates in the FZ and EDX (c and d) results for precipitates denoted by F1 and F2 of FSS weld made under FS8 (optimum) condition.

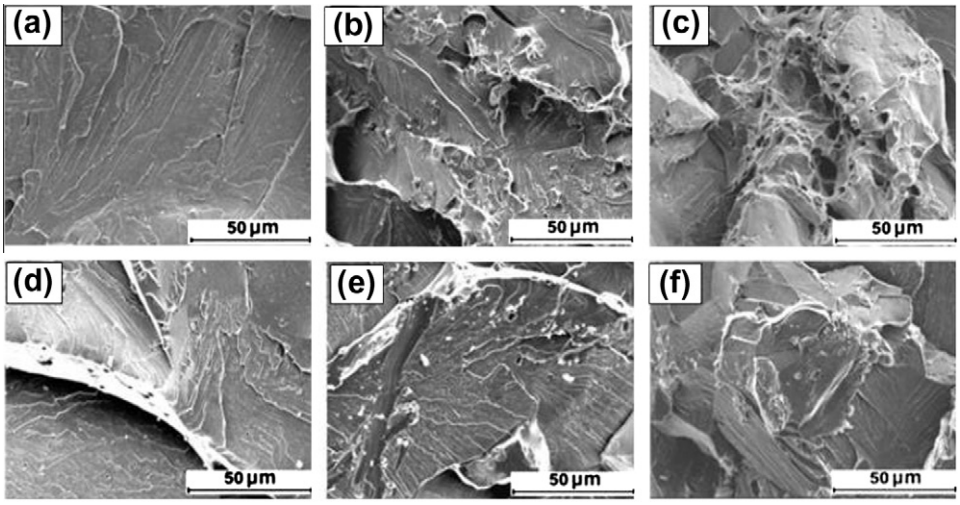

Fig. 14. Fractographs of tensile (a–c) and impact specimens (d–f) of FSS welds (a) FS4, (b) FS6, (c) FS8, (d) FS4, (e) FS6, (f) FS8.

3.3. Microstructure

Microstructures of all the joints were examined at the weld region of FSS welds and presented in Fig. 12. It is observed that the samples made at the optimum condition (i.e. $A_3B_2C_1$) resulted in fine equi-axed grains compared to other conditions. SEM was applied to observe the distribution of precipitates in the FZ of weldments made under optimum condition (i.e. $A_3B_2C_1$) and the results are presented in Fig. 13a and b. EDX is carried out to analyze the chemical compositions of the precipitations and the results were presented in Fig. 13c and d. From the EDX results, it is observed that the Ti, carbon compounds such as TiC [19] and Al_2O_3 were formed which are believed to be responsible for grain refinement. The austenite content in the weld region of FSS joints was measured in all the conditions of experimental layout and the results were presented in Table 5. From the results it is observed that the joints made under optimum condition (i.e. $A_3B_2C_1$) led to an increase in the austenite content. The increase in austenite content with the addition of Cu (3 g) at optimum condition can be attributed to the austenite stabilizing effect of Cu [33].

3.4. Fractography

The tensile and impact fracture surfaces of FSS weldments made at FS8 (Cu 3 g, Ti 2 g, Al 1 g), FS6 (Cu 2 g, Ti 3 g, Al 1 g) and FS4 (Cu 2 g, Ti 1 g, Al 2 g), conditions of experimental layout corresponding to optimum, medium and lower values of quality characteristics were analyzed by SEM to reveal the fracture surface morphology and the results are presented in Fig. 14. From the results it is observed that the fractured surfaces of weldments made under FS4 and FS6 conditions shows cleavage fracture indicating brittle failure, where as the tensile and impact fracture surfaces of welds made at optimum condition (i.e. $A_3B_2C_1$) shows quasi cleavage fracture indicating both ductile and brittle failure. This can be attributed to the equi-axed morphology of the FZ grains in the FSS welds [21].

4. Conclusions

The influence of grain refining elements such as Cu, Ti and Al on the microstructure, austenite content and mechanical properties of FSS welds were investigated and the following conclusions can be drawn.

(1) The same optimum combination (i.e. $A_3B_2C_1$) is observed in UTS, YS, %EL, IT, microhardness and austenite content of FSS welds. This is attributed to the solid solution strengthening by the formation of fine precipitates TiC and Al_2O_3 which are effective in promoting equi-axed grains and to refine the grain size in the WZ.
(2) The highest strength of welds at the optimum condition (i.e. $A_3B_2C_1$) without adversely affecting the ductility can be attributed to the highest percentage of retained austenite in the weld region.
(3) There is a marginal improvement in the ductility of FSS weldments at the optimum condition (i.e. $A_3B_2C_1$). This can be attributed to the equi-axed morphology of the FZ grains and formation of dimples, ductile voids in the WZ.
(4) The hardness was highest in the FZ of FSS weldments at the optimum condition (i.e. $A_3B_2C_1$). Maximum hardness in the FZ could be explained by the existence of fine precipitates TiC and Al_2O_3 and solid solution strengthening by the element Al during welding.

Acknowledgements

The authors would like to thank the authorities of Defence Metallurgical Research Laboratory (DMRL), Hyderabad, India and NIT, Warangal for providing the facilities to carry out this work. One of the authors (G. Mallaiah) is thankful to the Principal and the management of KITS, Huzurabad for their constant support during this work.

References

[1] Monypenny JHG. Stainless iron and steel. 3rd ed. London: Chapman and Hall Ltd.; 1954.
[2] Pickering FB. The metallurgical evolution of stainless steels. Int Met Rev 1976;1.
[3] Cary HB. Modern welding technology. New Jersey: Prentice-Hall; 1989.
[4] Hedge JC. Arc welding chromium steel and iron. Metal Prog 1935;27(4):33–8.
[5] Miller WB. Welding of stainless and corrosion resistant alloys. Metal Prog 1931;20(12):68–72.
[6] Amuda MOH, Mridha S. Grain refinement in ferritic stainless steel welds: the journey so far. Adv Mater Res 2010;83:1165–72.
[7] Reddy GM, Mohandas T. Welding aspects of ferritic stainless steels. Indian Weld J 1974;27(2):7.
[8] Dorschu KE. Weldability of a new ferritic stainless steel. Weld J 1971;50(9):408s.
[9] Kah DH, Dickinson DW. Weldability of ferritic stainless steels. Weld J 1981;60:135s.

[10] Brando WS. Avoiding problems when welding AISI 430 ferritic stainless steel. Weld Int 1992;6:713.
[11] Warmelo MV, Nolan D, Norrish J. Mitigation of sensitization effects in unsterilized 12% Cr ferritic stainless steel welds. Mater Sci Eng 2007;464A:157–69.
[12] Aksoy M, Yilmaz O, Korkut MH. The effect of strong carbide-forming elements on the adhesive wear resistance of ferritic stainless steel. Wear 2001;249: 639–46.
[13] Fujita N, Ohmura K, Yamamoto A. Changes of microstructures and high temperature properties during high temperature service of niobium added ferritic stainless steels. Mater Sci Eng 2003;351A:272–81.
[14] Sim GM, Ahn JC, Hong SC, Lee KJ, Lee KS. Effect of Nb precipitate coarsening on the high temperature strength in Nb containing ferritic stainless steels. Mater Sci Eng 2005;396A:159–65.
[15] Wang LX, Song CJ, Sun FM, Li LJ, Zhai QJ. Microstructure and mechanical properties of 12 wt.% Cr ferritic stainless steel with Ti and Nb dual stabilization. Mater Des 2009;30:49–56.
[16] Villafuerte JC, Kerr HW. Electromagnetic stirring and grain refinement in stainless steel GTA welds. Weld J 1990;69(1):1s.
[17] Reddy GM, Mohandas T. Explorative studies on grain refinement of ferritic stainless steel welds. J Mater Sci Lett 2001;20:721–3.
[18] Reddy GM, Mohandas T. Effect of frequency of pulsing in gas tungsten arc welding on the microstructure and mechanical properties of ferritic stainless steel welds. In: Symposium on joining of materials, WRI, Tiruchirapally; 1996. p. 105.
[19] Villafuerte JC, Pardo E, Kerr HW. The effect of alloy composition and welding conditions on columnar-equiaxed transitions in ferritic stainless steel gas tungsten arc welds. Metall Trans 1990;21A:2009–19.
[20] Villafuerte JC, Kerr HW, David SA. Mechanism of equiaxed grain formation in ferritic stainless steel gas tungsten arc welds. Mater Sci Eng 1995;194A: 187–91.
[21] Mohandas T, Reddy GM, Naveed MD. A comparative evaluation of gas tungsten and shielded metal arc welds of a ferritic stainless steel. J Mater Process Technol 1999;94:133–40.
[22] Ross PJ. Taguchi techniques for quality engineering. New York: McGraw-Hill; 1998. p. 24–98.
[23] Montgomery DC. Design and analysis of experiments. New York: Wiley; 1997. p. 395–476.
[24] Phadke MS. Quality engineering using robust design. Englewood Cliffs (NJ): Prentice-Hall; 1989.
[25] Kumar A, Sundarrajan S. Selection of welding process parameters for the optimum butt joint strength of an aluminium alloy. Mater Manuf Process 2006;21(8):789–93.
[26] Juang SC, Tarang YS. Process parameter selection for optimizing the weld pool geometry in tungsten inert gas welding of stainless steel. J Mater Process Technol 2002;122:33–7.
[27] Kumar A, Sundarrajan S. Effect of welding parameters on mechanical properties and optimization of pulsed TIG welding of Al–Mg–Si alloy. Int J Adv Manuf Technol 2008;42(1–2):118–25.
[28] Balasubramanian M, Jayabalan V, Balasubramanian V. Process parameter optimization of pulsed current argon tungsten arc welding of titanium alloy. J Mater Sci Technol 2008;24(3):423–6.
[29] Annual Book of ASTM Standards. Philadelphia, PA: American Society for Testing of Materials; 2004.
[30] Montgomery DC. Introduction to statistical quality control. 3rd ed. New York: John Wiley & Sons Inc.; 2001.
[31] Kumar A, Shailesh P, Sundarrajan S. Optimization of magnetic arc oscillation process parameters on mechanical properties of AA 5456 aluminum alloy weldments. Mater Des 2008;29(10):1904–13.
[32] Lakshminarayanan AK, Balasubramanian V, Reddy GM. On the fatigue behaviour of electron beam and gas tungsten arc weldments of 409M grade ferritic stainless steel. Mater Des 2011;35:760–9.
[33] Soylu B, Honeycombe RWK. Microstructural refinement of duplex stainless steels. Mater Sci Technol 1991;7(2):137–45.